

**PRODUCTION OF GAS-SOLID STRUCTURES IN ALUMINUM AND NICKEL  
ALLOYS BY GASAR PROCESSING**

V.I. Shapovalov\*, J.M. Apprill\*\*, M.D. Baldwin\*, M.C. Maguire\*\*\*, M.E. Miskiel\*

\*Sandia National Laboratories, P.O. Box 5800, MS 1134, Albuquerque, NM 87185-1134

\*\*University of Arizona, M.S.E. Dept., Tucson, AZ 85721

\*\*\*KomTek, 40 Rockdale St., Worcester, MA 01606

**Abstract**

Experimental data on directional and bulk solidification of hydrogen-charged samples of aluminum alloy A356 and nickel alloy Inconel 718 are discussed. The solidification structure of the porous zone is shown to be dependent on many process variables. Of these variables, hydrogen content in the melt prior to solidification, and furnace atmospheric pressure during solidification play the decisive role. Also important are the furnace atmosphere composition, the solidification velocity, and the temperature distribution of the liquid metal inside the mold.

## **DISCLAIMER**

This report was prepared as an account of work sponsored by an agency of the United States Government. Neither the United States Government nor any agency thereof, nor any of their employees, make any warranty, express or implied, or assumes any legal liability or responsibility for the accuracy, completeness, or usefulness of any information, apparatus, product, or process disclosed, or represents that its use would not infringe privately owned rights. Reference herein to any specific commercial product, process, or service by trade name, trademark, manufacturer, or otherwise does not necessarily constitute or imply its endorsement, recommendation, or favoring by the United States Government or any agency thereof. The views and opinions of authors expressed herein do not necessarily state or reflect those of the United States Government or any agency thereof.

## **DISCLAIMER**

**Portions of this document may be illegible in electronic image products. Images are produced from the best available original document.**

## Introduction

It has been shown that a gas-eutectic equilibrium may occur in binary metal-hydrogen systems in the vicinity of the melting temperature of the pure metal [1]. This happens mainly in systems where no formation of metal hydrides occur at high temperatures, such as Fe-H, Cu-H, Ni-H, Al-H, and Mg-H. When the metal is charged with hydrogen to a level near the gas-eutectic concentration, solidification involves the transformation of the liquid to a solid and a gaseous phase and a variety of gas-solid structures may develop [2]. This transformation is termed *gas-eutectic* and the process to produce gas-solid structures is termed the *Gasar process* [3]. Of particular interest is *gasarite*, a structure featuring an ordered porous region [2]. Materials possessing this structure, or *Gasars*, display mechanical properties superior to porous materials produced by other methods. While gasarite is more or less readily obtained in binary metal-hydrogen systems, it may only form under special conditions in ternary or more complex alloys where no explicit gas-eutectic equilibrium is attained.

Producing Gasars from complex, high-strength alloys with mechanical properties exceeding those of the pure base metal is of great interest for commercial applications. No consistent experimentation in this area has been performed. The major reason being the notorious difficulties of working with hydrogen at high temperatures.

The purpose of this study was to examine the gas-solid solidification structure of the widely used aluminum alloy A356, and nickel alloy Inconel 718. The basic thermodynamic data were obtained previously [4]. Alloy A356 is widely used in aerospace applications; hence, the desire to reduce its density by 40-50 % without appreciably compromising its tensile strength (as demonstrated by previous work on copper and magnesium Gasars [5]). Inconel 718 combines favorable mechanical properties with outstanding resistance to corrosion, particularly at high temperatures. However, its high density ( $8.22 \text{ g/cm}^3$ ) severely restricts its applications in aerospace vehicles, so reducing the density of this alloy is likewise attractive.

## Experiments and Results

Commercial alloy samples were used in the experimentation. The composition of the A356 cast bars was 5.86 % Mg, 0.13 % Ti, 0.2 % Fe, balance Al. Inconel 718 was supplied in 12 mm rolled bars with chemical composition: 5.2 % Nb, 3.1 % Mo, 0.9 % Ti, 0.5 % Al, balance Ni. Hydrogen and argon of technical-grade purity were used as components of the controlled atmospheres. No special purification was carried out. A mechanical vane pump was used at the roughing stage to provide a vacuum of 10 to 50 millitorr. All experimentation was performed at the Liquid Metals Processing Laboratory of Sandia National Laboratories, Albuquerque, New Mexico. The details of this unit have been described elsewhere [4]. The partial pressures of hydrogen and argon were varied from 0.01 to 2.0 MPa. The temperature was measured by a W-Re thermocouple. During the A356 experiments the thermocouple was protected by an alumina sheath and introduced into the melt. During the Inconel 718 experiments, the thermocouple was placed within the stopper rod, 50 mm from the crucible bottom. A two color optical pyrometer was used as a back-up in case of thermocouple malfunction. The melting process was monitored by an external video camera aimed at the crucible and solidification was observed with an internal video camera aimed at the mold.

Charge weight was 2 to 5 kg for the A356 experiments and 4 to 9 kg for the Inconel 718 experiments. The castings were subjected to density measurements by hydrostatic weighing (Archimedes principle), then cut across their structural zones to determine the local void fractions and pore morphology. In some cases, microstructural characterization and chemical analyses were performed. Two solidification modes were investigated, namely directional solidification and bulk solidification.

The directional solidification experiments involved the following steps:

- heating and melting the charge in a controlled atmosphere,
- 10 minute soak of the melt at constant temperature and partial pressures of the gases,
- tapping the melt into a cylindrical mold 165-250 mm in diameter having a copper base and ceramic walls, and
- solidification under controlled— varied or constant — pressure.

The velocity of directional solidification was varied by changing the thickness of the ceramic coating on the copper base, the water flow velocity in the copper chill, and the tapping temperature.

The bulk solidification experiments involved the following steps:

- heating and melting the charge in a controlled atmosphere,
- 10 minute soak of the melt under constant conditions,
- cooling the alloy down to, or slightly below, its liquidus temperature,
- tapping the melt into a ceramic mold minimizing heat losses, and
- varying gas pressure above the melt at a preset rate during solidification.

The major process variables in this series of experiments were the pressure variation rate during solidification, the solidification velocity, the tapping temperature, and the rate of melt cool-down to liquidus temperature.

## Alloy A356

### Directional Solidification

The directional solidification experiments of A356 resulted in a macrostructure featuring two zones, Fig. 1. Compact spheroidal pores having relatively small diameters, 0.1 to 2.0 mm, occur in the bottom zone that adjoins the copper base. The pore diameter increases by a factor of 2 to 3 from bottom to top. The pores show a uniform, although not ideal, frequency distribution throughout the zone. At the top of the casting there is another zone of large gas holes whose shape is replicated at the casting surface.

The void fraction values averaged across the casting and within the bottom zone are mainly dependent on the hydrogen pressure, the holding temperature, and the gas pressure during solidification. All other process variables exert much less control. The solidification pressure has an especially marked effect, Fig. 2. Yet the influence of pressure is not uniform over its entire range. Above 0.04 MPa, its effects are hardly observable. Conversely, even minute pressure variations within the range from 0.005 to 0.01 MPa lead to dramatic changes

in the void fraction. This is the cause of the broad scatter in the lower pressure range. Fig. 2 shows an abrupt rise in Gasar void fraction as the pressure is lowered below 0.02 MPa. However, the void fraction, even in successful directional solidification runs, did not exceed 30 percent.

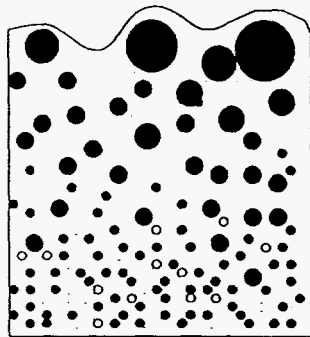


Figure 1. Schematic of directionally solidified A356 Gasar macrostructure.

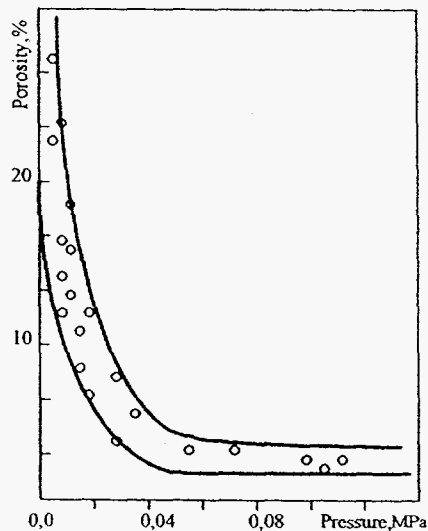


Figure 2. Influence of solidification pressure on void fraction of directionally solidified A356 Gasar ingots. Hydrogen charging pressure 0.5 MPa, charging and pouring temperature 900 °C.

### Bulk Solidification

The bulk solidification experiments normally resulted in spheroidal pores, although compact pores of complex shape also formed, Fig. 3. The distribution of pores across the casting was much more intricate than in directionally solidified ingots and was dependent on the temperature distribution in the melt at the instance of pressure change. This factor was found to be highly important because it determined conditions of hydrogen bubble nucleation and growth. When a region was too cold, bubbles grew slower than the solid, making the region lean in porosity. When the local temperature was too high, the bubbles grew more rapidly than the solid, expanded significantly, and floated up to the melt surface. As a result, a

low-porosity material formed in the overheated melt region as well. Therefore, various macrostructures could develop when no special measures were taken to equalize the melt temperature throughout the casting, Fig. 3.

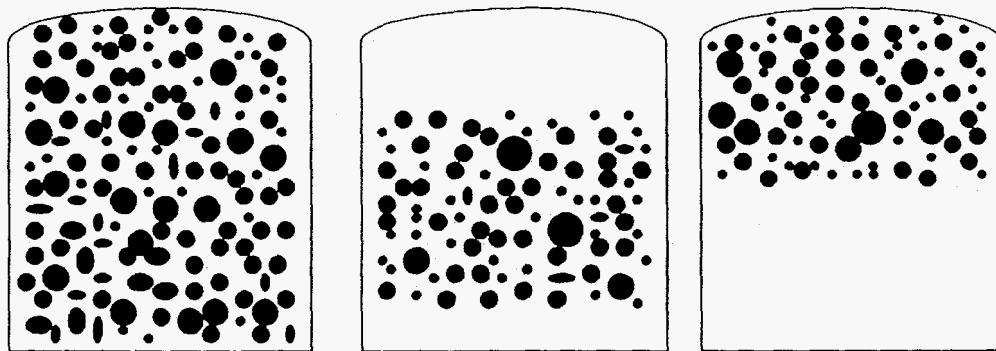


Figure 3. General macrostructural types of bulk-solidified A356 Gasar ingots. Left: uniform temperature distribution in the melt. Rest: nonuniform temperature distribution.

Both the overall and local void fractions were greater in the bulk solidified materials than in the directionally solidified ones. The major factors affecting void fraction were the pressure difference between the holding and the solidification step, the melt tapping temperature, and the rate of melt cool-down to the liquidus temperature.

Worthy of special mention are pore dimensions and shape. The average pore size ranged from 0.5 to 10 mm, depending on the terminal pressure and the starting temperature of pressure decline during solidification. Titanium additions also played a part, for they enhanced hydrogen solubility in the melt and facilitated gas bubble nucleation. The latter effect is associated with the formation of fine particles of refractory intermetallic  $TiAl_3$ . These have a very low surface energy and act as bubble nucleation sites when the pressure is reduced. Microstructural characterization revealed that the  $TiAl_3$  crystals have a plate-like shape and are predominantly found at the hydrogen bubble surface. The hydrogen bubbles adhere to the aluminide particles rather strongly, so that the thermodynamic impetus for and the rate of bubble coalescence are markedly reduced. Also hindered is mechanical removal of bubbles from the solidifying melt via upward floatation. As a result, the final void fraction is further increased. The maximum void fraction achieved by bulk solidification was 78 percent, with the pores having a complex compact shape and an average size of 4 to 8 mm.

## Inconel 718

### Directional Solidification

The directional solidification of hydrogen-charged Inconel 718 results in a macrostructure generally featuring four zones. Aligned, columnar pores make a honeycomb structure in the casting bottom section that contacts the water-cooled chill, Fig. 4. A relatively shallow zone of coarse pores, sometimes coalesced to form disk-shaped cavities, is found above the bottom zone. This results from coalescence of neighboring pores as they grow in

the honeycomb zone, so the region in question is termed the coalescence zone. Above this, a zone of more or less compact pores having complex dendrite-like shapes is revealed. Further, the top portion of the casting is where large subsurface bubbles (pores) concentrate. The overall void fraction of the honeycomb zone was approximately equal to that of the coalescence zone and ranged from 5 to 67 %, depending on the Gasar process variables. The void fraction was primarily affected by the hydrogen charging pressure and the argon pressure during solidification. The absolute and relative dimensions of the zones are also dependent on conditions of melting and solidification. It is possible to produce castings having only one of the above zones or any combination of two or three of them. To do this, however, the mold shape and material and the sample weight sometimes have to be changed. For example, the copper base was in some cases replaced by non-cooled slabs of graphite, ceramic, or steel, 25 mm thick.

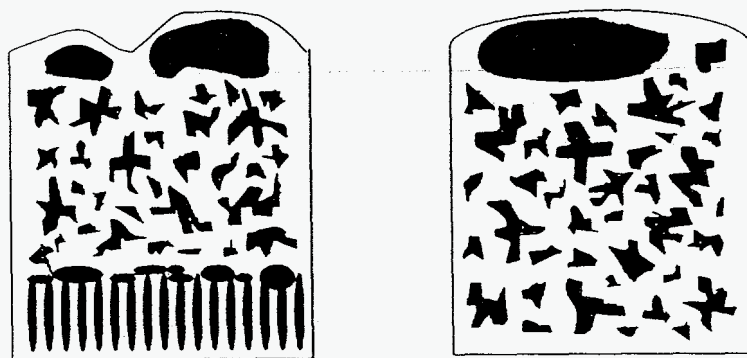


Figure 4. Schematics of Alloy 718 Gasar ingot macrostructure produced by directional (left) and bulk solidification (right).

“Twin-plate” casting was performed using two similar or dissimilar plates spaced 1 to 25 mm apart. The cooling plate material affected the Gasar structure and void fraction fairly strongly. It was always possible, however, to select pressures of hydrogen and argon and tapping temperature so that a desired structure and void fraction (up to 65 %) could be achieved in cast sheets up to 25 mm thick. In-situ production of sandwich constructions with Inconel 718 is thus feasible. Such Gasar sheets 1 to 2 mm thick with an overall void fraction of approximately 45 % may consist of a porous core and two nonporous skins.

#### Bulk Solidification

The bulk solidification experiments resulted in the formation of only two structural zones, Fig. 4. The major part of the casting was occupied by a region of fairly coarse, dendrite-shaped pores. Practically no honeycomb zone was found. The overall void fraction turned out to be slightly greater than that obtained by directional solidification. Although somewhat surprising, this finding lends itself to an explanation. First, the surface energy of nickel is much greater than that of aluminum, so the hydrogen bubbles are much more apt to coalesce in Inconel 718 than they are in aluminum. It should be remembered that the velocity of bubble flotation increases with the bubble size. Second, the buoyancy force acting on a hydrogen bubble of a given size in the nickel alloy is three times that of the buoyancy force in the aluminum base alloy. The bubbles therefore tend to rise much more rapidly and the



hydrogen escapes the melt and/or the mushy zone more quickly before solidification is completed in the nickel alloy.

It should be noted that the gas-solid structure formation in bulk solidification is not completely understood. More in-depth studies are needed to determine the effects of such factors as the temperature at which reducing the pressure is started, the rate of pressure reduction, and the rate of temperature reduction down to the liquidus temperature. These issues, however, have fallen outside the scope of the present study.

### Conclusions

Gasars from Al A356 may be produced by both directional and bulk solidification. In both cases, however, attempts to obtain a honeycomb structure have not met with success.

With no special additives, aluminum alloy Gasars can only be made by solidification under pressures below 1 atm. Additives reducing the energy at the hydrogen-solid metal interface facilitate nucleation and individual growth of gas bubbles. This enhances the void fraction, makes the results more consistent, and enables Gasar synthesis via solidification at and above 1 atm pressure.

Gasars from Inconel 718 produced by directional solidification contain a honeycomb type structure with void fractions up to 65 % in layers up to 25 mm thick. No honeycomb morphology is observed in bulk solidification which results in a peculiar dendrite-like pore shapes.

### Acknowledgments

The present writers are indebted to Frank Zanner who initiated Gasar research at Sandia National Laboratories, to William Hammeter and James Maroone whose managerial support provided the necessary resources for this effort, and to Leif Gonnsen, Sam Giron and Greg Shelmidine of the Liquid Metals Processing Laboratory for their steady help and support.

### References

1. V.I.Shapovalov, Effects of Hydrogen on Structure and Properties of Fe-C Alloys, Metallurgy Publishing House, Moscow, 1982.
2. V.I.Shapovalov, Formation of Ordered Gas-Solid Structures Via Solidification in Metal-Hydrogen Systems, MRS Symposium Proceedings V. 521, Porous and Cellular Materials for Structural Applications. Symp. Held April 13-15, 1998, San Francisco, California, U.S.A. Editors: D.Schwartz, D.Shih, A.Evans, H.Wadey, 1998, p.p.281-290.
3. V.I.Shapovalov, Method for Manufacturing Porous Articles, U.S.Patent No.5181549, Jan.1993.

4. M.D.Baldwin, M.C.Maguire, F.J.Zanner Anisotropic Porous Metals Production by Melt Processing., Proceedings of the 1997 International Symposium on Liquid Metal Processing and Casting, Santa Fe, New Mexico, February 16-19, 1997. Editors: A.Mitchell and P.Auburtin.1997, p.p.417-425.
5. A.E.Simon and L.J.Gibson, Acta Mater. Vol. 44, No.4, p.1437-1449, 1996.